



A PDF micromixing model of dispersion for atmospheric flow. Part II: application to convective boundary layer

M. Cassiani^{a,*}, P. Franzese^b, U. Giostra^a

^a*Facoltà di Scienze Ambientali, campus scientifico Sogesta, Università di Urbino, Urbino 61029, Italy*

^b*School of Computational Sciences, George Mason University, Fairfax, Virginia 22030, USA*

Received 5 April 2004; received in revised form 5 November 2004; accepted 17 November 2004

Abstract

The Lagrangian stochastic probability density function (PDF) model developed by Cassiani et al. [Atmos. Environ. (2005) Part 1] is extended to the atmospheric convective boundary layer. The model is applied to simulate concentration statistics and PDF generated by passive releases from point and line sources in the convective boundary layer. A dynamical time-expandable grid is implemented, which optimises the computational resources required for dispersion simulations in atmospheric flow. A parameterised formulation for the micromixing time scale in convective conditions is derived. Model concentration statistics including mean field, fluctuations and concentration PDF are tested with four water tank experiments.

© 2004 Elsevier Ltd. All rights reserved.

Keywords: Concentration fluctuations; Micromixing modelling; Monte Carlo simulation; Turbulent dispersion; Chemical reactions

1. Introduction

Lagrangian stochastic (LS) models are an effective modelling tool for the prediction of the mean concentration field of passive scalars in the atmospheric convective boundary layer (CBL). Recently, LS models have been expanded to predict all moments of concentration using a fluctuating plume approach (Luhar et al., 2000; Cassiani and Giostra, 2002; Franzese, 2003) based on parametric forms for the relative particle spread and for the relative intensity of concentration fluctuations. A different technique based on LS modelling coupled with probability density function (PDF) methods and a dynamical grid formulation was presented and tested

in homogeneous turbulence and in the atmospheric neutral boundary layer by Cassiani et al. (2005). The PDF model still uses a parameterised relative spread indirectly, but does not use relative concentration fluctuations as an input. This paper describes an application of this technique to the simulation of passive scalar dispersion in the CBL.

The model uses the dynamical grid formulation to predict concentration statistics and the full one-point concentration PDF. The definition of the micromixing time scale used in Cassiani et al. (2005) was adapted to account for the turbulence characteristics and the domain structure of the CBL. Luhar and Sawford (2005) describe a similar application of PDF modelling to the CBL using a fixed computational grid, sequential simulation of particles, a mean concentration field pre-computed by a preliminary release of marked particle and a slightly different definition of the micromixing time scale.

*Corresponding author. Tel.: +39 0722 304249; fax: +39 0722 304265.

E-mail address: massimo.cassiani@uniurb.it (M. Cassiani).

The present model can be extended to account for chemical reactions with no additional closure assumptions. The inclusion of chemical reactions is straightforward because the model evolution equations for velocity, position and concentration are solved in parallel for all sampled particles. The model ability to simulate the releases of reactive substances is a desirable option because most of the chemical reactions involving reactive contaminants take place in daytime, when unstable conditions generated by convective turbulence are a typical occurrence for low winds, with strong inhomogeneous turbulence in the vertical direction.

The model equations and the turbulence input statistics are described in Section 2. A standard LS model (Luhar and Britter, 1989) has been used to model the trajectories of the particles, while the evolution of the concentration of each individual particle is governed by an interaction by exchange with the conditional mean (IECM) micromixing model (Fox, 1996). The turbulence statistics input into the model have been selected fitting the observations from the experiment of Deardorff and Willis (1985); the same parameters have been used for all simulations reported in this paper, including the comparisons with the experiments of Willis and Deardorff (1978), Deardorff and Willis (1984), Hibberd (2000) and Weil et al. (2002).

In Section 3, a short discussion and a definition of the dissipation time scale for CBL used by the IECM model is presented. The dissipation time scale has been defined as a function of relative particle spread and standard deviation of relative velocity. Model simulation results for point and line sources are reported in Section 4 along with comparisons with the experiments. Limitations and the potential future development of the model are discussed in the conclusions.

2. Model equations

The set of stochastic differential equations describing the evolution of velocity, position and concentration of a particle is

$$dU_i = a_i(\mathbf{X}, \mathbf{U}, t) dt + b_{ij}(\mathbf{X}, \mathbf{U}, t) d\zeta_j, \quad (1)$$

$$dX_i = U_i dt, \quad (2)$$

$$dC = \varphi(C, \mathbf{X}, \mathbf{U}, t) dt, \quad (3)$$

where the capital letters indicate quantities associated to the particle (i.e. Lagrangian quantities). \mathbf{U} is the particle velocity vector, \mathbf{X} is the particle position vector and C is the concentration associated with the particle. $d\zeta_j$ indicates a vector of independent Wiener processes with zero mean and variance dt (e.g., Gardiner, 1983). The mean wind is assumed to be known; therefore we will refer to the turbulent velocities as the velocity field,

where the principal direction 1 coincides with the mean wind direction. Thus, the mean components of the velocity vector \mathbf{u} in the two transverse directions are zero, and in these directions we do not need to distinguish further between u_i and $u_i - \langle u_i \rangle$. For instance, $\sigma_{u_i}^2 = \langle u_i^2 \rangle$ for $i = 2, 3$. The Taylor translation hypothesis $x = \langle \mathbf{u} \rangle t$ is used to reduce the problem from three to two dimensions. This is a good approximation in the CBL since the mean wind is usually $1.2w_* < |\langle \mathbf{u} \rangle| < 6w_*$. When it is more convenient we will use the classical meteorological notation $(x, y, z) = (x_1, x_2, x_3)$ and $(u, v, w) = (u_1, u_2, u_3)$ instead of the indicial notation.

2.1. The lagrangian stochastic model for velocity and position

The terms a_i and b_{ij} in Eq. (1) jointly model the effect of viscous stresses and pressure gradient on the evolution of the joint velocity and concentration PDF. The coefficient $b_{ij}(\mathbf{X}, \mathbf{U}, t)$ is obtained by imposing consistency with the Lagrangian structure function in the inertial subrange, i.e. $b_{ij} = \delta_{ij}(C_0\varepsilon)^{1/2}$, where C_0 is the Kolmogorov constant and ε is the mean dissipation of turbulent kinetic energy.

The coefficient $a_i(\mathbf{X}, \mathbf{U}, t)$ is obtained by ensuring the fulfilment of the well-mixed condition (Thomson, 1987), see also Cassiani et al. (2005). The two-dimensional PDF of crosswind velocities is written as $f_{\mathbf{u}} = g_v \psi_w$, where g indicates a Gaussian function, i.e. $g_v = \exp[-v^2/(2\sigma_v^2)]/\sqrt{2\pi\sigma_v^2}$, and ψ_w is assumed to be the sum of two Gaussians, i.e. $\psi_w = A_s g_s + A_d g_d$ (e.g., Baerentsen and Berkowicz, 1984). g_s and g_d are related to the PDFs of updraft and downdraft velocity, respectively, and A_s and A_d are related to the updraft and downdraft area, respectively (Luhar and Britter, 1989).

With these definitions and assuming that σ_v is homogeneous in the vertical direction the equation for the horizontal crosswind velocity is simply

$$dV = -\frac{C_0\varepsilon}{2\sigma_v^2} V dt + (C_0\varepsilon)^{1/2} d\zeta. \quad (4)$$

The particle vertical velocity W will be modelled according to Luhar and Britter (1989), i.e.

$$dW = a(z, W) dt + (C_0\varepsilon)^{1/2} d\zeta_3 \quad (5)$$

with

$$a(z, W) = (2\Phi - C_0\varepsilon Q)/(2\psi_w),$$

$$g_s = \exp[-(W - m_s)^2/(2\sigma_s^2)]/\sqrt{2\pi\sigma_s^2},$$

$$g_d = \exp[-(W + m_d)^2/(2\sigma_d^2)]/\sqrt{2\pi\sigma_d^2},$$

where m_s is the mean updraft velocity, m_d is the absolute value of the mean downdraft velocity and σ_s^2 and σ_d^2 are the updraft and downdraft variance, respectively. Following Baerentsen and Berkowicz (1984), $\sigma_s = m_s$ and $\sigma_d = m_d$ with

$$m_s = \sigma_w^2 / (2m_d),$$

$$m_d = \left(\sqrt{\langle w^3 \rangle^2 + 8\sigma_w^6} - \langle w^3 \rangle \right) / (4\sigma_w^2),$$

$$A_s = m_d / (m_d + m_a),$$

$$A_d = m_s / (m_d + m_a),$$

$$Q = g_s A_s (W - m_s) / m_s^2 + g_d A_d (W + m_d) / m_d^2$$

and

$$\begin{aligned} \Phi = & -\frac{1}{2} \left(A_s \frac{\partial m_s}{\partial z} + m_s \frac{\partial A_s}{\partial z} \right) \operatorname{erf} \left(\frac{W - m_s}{\sqrt{2} m_s} \right) \\ & + m_s \left[A_s \frac{\partial m_s}{\partial z} \left(\frac{W^2}{m_s^2} + 1 \right) + m_s \frac{\partial A_s}{\partial z} \right] g_s \\ & + \frac{1}{2} \left(A_d \frac{\partial m_d}{\partial z} + m_d \frac{\partial A_d}{\partial z} \right) \operatorname{erf} \left(\frac{W - m_d}{\sqrt{2} m_d} \right) \\ & + m_d \left[A_d \frac{\partial m_d}{\partial z} \left(\frac{W^2}{m_d^2} + 1 \right) + m_d \frac{\partial A_d}{\partial z} \right] g_d. \end{aligned}$$

For a crosswind line source, only Eq. (5) for the vertical component of velocity is required.

Luhar and Britter (1989) showed that this model correctly reproduces the mean field observed in Willis and Deardorff (1976, 1978, and 1981) water tank experiments. It is possible to use other LS models, such as, for example, a model using the closure introduced in Luhar et al. (1996), or the model described in Franzese et al. (1999).

Perfect reflection of particle positions at the boundaries was used. The reflected velocities are randomly extracted from the positive part of the updraft velocity PDF and from the negative part of the downdraft velocity PDF (g_s and g_d , respectively), depending on which boundary is reflecting the particle. Simple testing of this scheme (not reported here) showed negligible errors in the simulated well-mixed distribution of particles at large time. Once the computational domain reaches the physical boundary the velocity skewness goes to zero and perfect reflection for both position and velocity is used. More refined boundary conditions in non-Gaussian turbulence are discussed in Thomson and Montgomery (1994); however, their implementation may be laborious and computationally intensive when an expanding domain is used (Cassiani et al., 2005).

2.1.1. Input turbulence statistics

The vertical profiles of the variance of the three velocity components and of the energy dissipation are

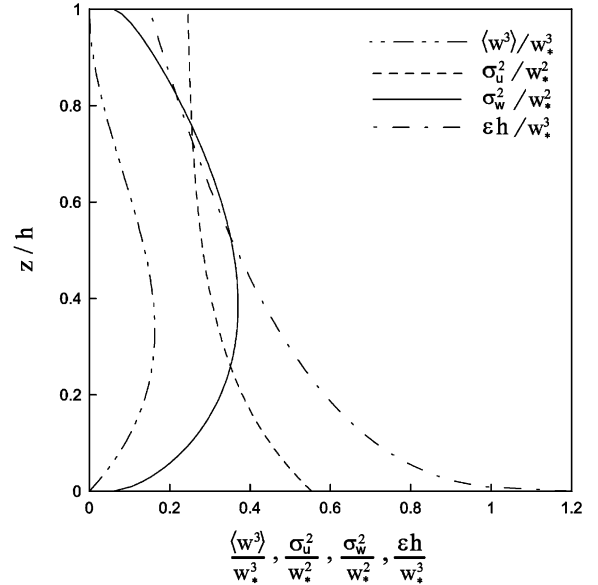


Fig. 1. Dimensionless input turbulence statistics as a function of the vertical coordinate scaled with the boundary layer height h .

parameterised fitting the data from the tank experiment reported in Deardorff and Willis (1985):

$$\sigma_w^2 = w_*^2 \{ 0.06 + [(z/h)(1 - 0.7z/h)(1 - z/h)]^{2/3} \},$$

$$\sigma_u^2 = w_*^2 \{ 0.24 + \exp[-4(z/h + 0.29)] \},$$

$$\sigma_v^2 = 0.2w_*^2,$$

$$\varepsilon = w_*^3 [1.2 - 1.05(z/h)^{1/3}] / h.$$

The third moment of the vertical velocity is the same as the one used by Franzese et al. (1999): $\langle w^3 \rangle = 1.1w_*^3(z/h)(1 - z/h)^2$. The above input profiles of σ_w^2/w_*^2 , σ_u^2/w_*^2 , $\varepsilon h/w_*^3$ and $\langle w^3 \rangle/w_*^3$ are reported in Fig. 1. This set of inputs was used in all our comparisons with the Willis and Deardorff (1978), Deardorff and Willis (1984), Hibberd (2000) and Weil et al. (2002) experiments.

2.2. Micromixing model

The coefficient φ in Eq. (3) is specified according to the IECM model of Fox (1996)

$$\frac{dC}{dt} = \frac{1}{t_m} (C - \langle c | \mathbf{X}, \mathbf{U} \rangle), \quad (6)$$

where $\langle c | \mathbf{X}, \mathbf{U} \rangle$ is the ensemble mean concentration conditioned on the particle position vector and on the particle velocity vector. The dissipation time scale t_m will be defined in the next section. The accuracy of the estimated ensemble mean for the location and velocity of

the particles can be assessed based on the standard criteria for Monte Carlo statistical methods and depends on the number of sampled particles (Cassiani et al., 2005).

The calculation of concentration statistics are based on the dynamical time-expandable grid described in Cassiani et al. (2005). The stochastic differential equations for velocity (1) and position (2) are discretized using a simple Euler scheme, whereas the IECM Eq. (3) is discretized as

$$C(t + \Delta t) = C(t) - \left\{ 1 - \exp\left(-\frac{1}{t_m} \Delta t\right) \right\} (C(t) - \langle c | \mathbf{X}, \mathbf{U} \rangle). \quad (7)$$

3. Definition of the dissipation time scale in a convective boundary layer

The dissipation time scale t_m in Eq. (6) is defined as discussed in Cassiani et al. (2005), following the semi-empirical formulation of Sawford (2004): $t_m = \mu \sigma_r / \sigma_{ur}$ at short and intermediate time from the release, where μ is an empirical constant to be evaluated, σ_r is the instantaneous plume spread which is assumed as a characteristic length scale of the scalar field and $\sigma_{ur} = \langle u_r^2 \rangle^{1/2}$ is the root mean square of the relative velocity fluctuations. u_r indicates the difference between a component of the particle turbulent velocity and the corresponding component of the velocity of the instantaneous centre of mass of the plume. Thus, σ_{ur}^2 represents the fraction of turbulent energy contributing to the instantaneous relative plume spread, and is modelled according to Franzese (2003):

$$\sigma_{ur}^2 = \sigma^2 \left(\frac{\sigma_r}{L} \right)^{2/3}, \quad (8)$$

where σ^2 is assumed to be the average of the variances of the three components of velocity, i.e. $\sigma^2 = (\sigma_u^2 + \sigma_v^2 + \sigma_w^2)/3$ and L is a characteristic length scale of the most energetic eddies which is assumed to be equal to the CBL height, i.e. $L = h$. The plume relative spread is parameterised as

$$\sigma_r^2 = \frac{d_r^2}{1 + (d_r^2 - \sigma_0^2)/(\sigma_0^2 + 2\sigma^2 T_L t)}, \quad (9)$$

where d_r^2 is the inertial range variance of the one-dimensional distribution of particles around the instantaneous centre of mass of the plume, i.e. $d_r^2 = C_r \varepsilon (t_0 + t)^3$, with $t_0 = [\sigma_0^2 / (C_r \varepsilon)]^{1/3}$ (Franzese, 2003). $C_r = 0.3$ as in Cassiani et al. (2005), in agreement with the experimental results of Hibberd (2000) as reported in Luhar et al. (2000). Eq. (9) ensures that σ_r is consistent with the inertial range formulation and tends to the Taylor diffusion limit at large time, i.e. $\sigma_r = \sigma_0$ as $t \rightarrow 0$;

$\sigma_r = d_r$ for $t_s \ll t \ll T_L$; and $\sigma_r = \sqrt{2\sigma^2 T_L t}$ for $t \gg T_L$; σ_r is constrained to not exceed the boundary layer height. Because the turbulence is not homogeneous in the vertical direction, σ^2 and ε are local quantities which depend on the particle vertical position. Therefore the numerical procedure described in Cassiani et al. (2005) is used to evaluate σ_r for each particle and the value of t_m for each cell. The calculated t_m depends on both the downwind distance from the source and the vertical position of the particle. The constant μ was determined from the best fit of model results to the tank data. In the simulations of a crosswind line source we used $\mu = 0.8$; for a continuous point source $\mu = 0.7$.

4. Comparisons with the experiments

The model was tested with the data from four experiments of dispersion in the CBL: Willis and Deardorff (1978), Deardorff and Willis (1984), Hibberd (2000) and Weil et al. (2002).

All of the above are water tank experiments. In the Hibberd (2000) experiments the convective turbulence was simulated by saline convection (Hibberd and Sawford, 1994); in the other experiments the turbulence was driven by heat generated convection.

The crosswind-integrated mean concentration field simulated by the model for elevated sources is compared with the observations from the experiments of Willis and Deardorff (1978) for a source height $z_s = 0.24h$, and Hibberd (2000) for $z_s = 0.25h$. The experiments were conducted for a continuous release from a crosswind line source, with zero horizontal and vertical momentum.

The Taylor translation hypothesis is used to transform the time into downwind distance from the source, i.e. $x = \langle u \rangle t$ where $\langle u \rangle$ is the mean wind speed which is assumed to be constant along the boundary layer vertical direction. The simulation is thus reduced to one dimension. The initial spread of the simulated plume was taken equal to the source diameter in the Hibberd (2000) experiment, i.e. $\sigma_0 = 6.7 \times 10^{-3} h$. However, σ_0 has a small effect on the simulated mean concentration field.

Fig. 2 shows the contour lines of the crosswind-integrated mean concentration $\langle c \rangle_y = \int_{-\infty}^{\infty} \langle c \rangle dy$ scaled with the crosswind-integrated well-mixed concentration. Contour lines are plotted as a function of the dimensionless downwind distance, $X = w_* x / (\langle u \rangle h)$, and of the dimensionless vertical coordinate z/h . Because the two experiments show very similar mean concentration fields, we report only the simulation for $z_s = 0.25h$. The simulated contour lines capture the essential features of the field with a good agreement especially on the lower half of the domain. The agreement worsens in the upper half of the domain, especially near the upper boundary.

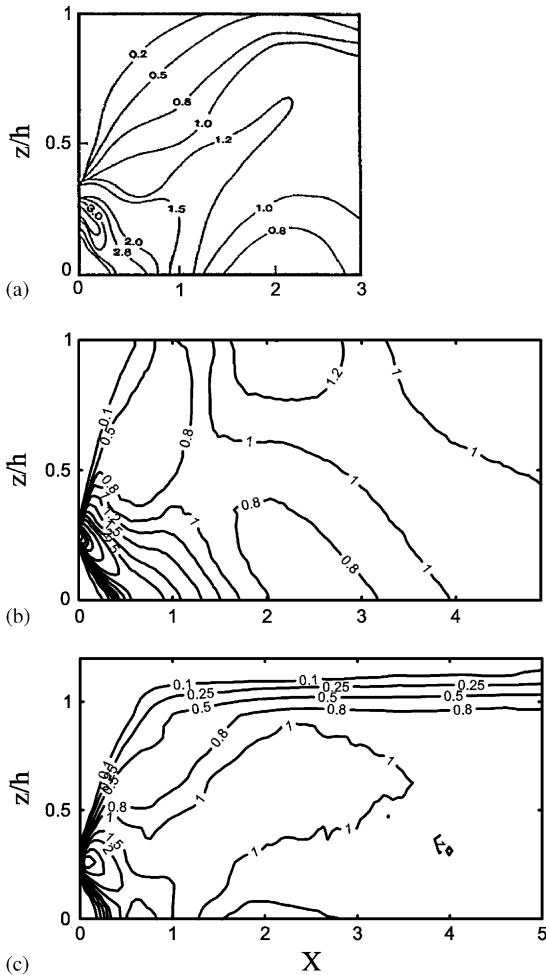


Fig. 2. Contours of dimensionless crosswind mean concentration as function of dimensionless vertical coordinate z/h and dimensionless downwind distance X . (a) Willis and Deardorff (1978) experiment; (b) model simulation; (c) Hibberd (2000) experiment.

This is due to the simple reflection conditions used in the model, where the upper boundary is assumed to be an idealised reflective barrier. In the experiments, the upper boundary is a region of low permeability that extends from about $0.9h$ to about $1.2h$, and the exchange of fluid through the boundary creates the observed gradient of mean concentration near the top. In fact, this phenomenon is a more realistic representation of the exchange processes at the top of the atmospheric boundary layer than the modelled perfect reflection.

The measured and modelled crosswind-integrated ground level concentration scaled by the well-mixed concentration, GLC_y , are shown in Fig. 3. GLC_y measured in Willis and Deardorff (1978), in Deardorff and Willis (1984); $z_s = 0.22h$ and in Hibberd (2000), are

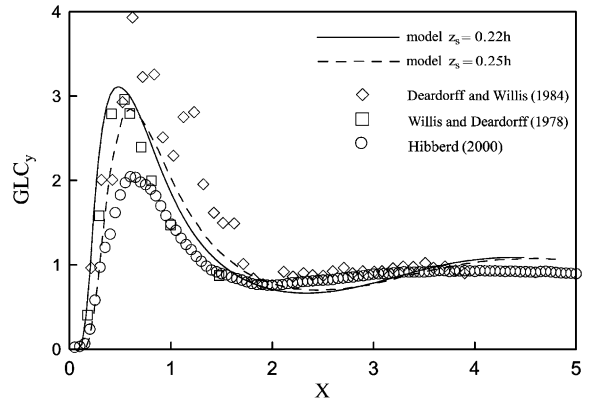


Fig. 3. Dimensionless crosswind ground level concentration GLC_y measured (open symbols) and modelled (lines). X is the dimensionless downwind distance and z_s the source elevation.

quite different, showing the GLC_y sensitivity to the details of the experiment. The ratio of stack exit velocity to mean wind speed in the Deardorff and Willis (1984) non-buoyant plume experiment was about five. Because of the plume initial momentum, the release can be regarded as a jet in a convective turbulent cross flow. However, an effective source height was estimated by Luhar et al. (2000) to be approximately $0.22h$, which is the value we used in our simulation. This value is consistent with the downwind location of the maximum GLC_y measured in this experiment, which is approximately the same as in Willis and Deardorff (1978) and Hibberd (2000) experiments. The simulated max GLC_y show a fair overall agreement with the observations. The location of the maximum at $X \sim 0.6$ and the presence of a local minimum at $X \sim 2$ in all the experiments are captured by the model with a good approximation.

The intensity of concentration fluctuations $\sigma_c/\langle c \rangle$ simulated by the model for a release height of $0.25h$ is compared with the observations from the Hibberd (2000) experiments in Fig. 4. Fig. 4(a) shows $\sigma_c/\langle c \rangle$ as a function of X at the vertical position of the plume centre of mass; Fig. 4(b) reports the observed and measured ground level $\sigma_c/\langle c \rangle$. The shape of the observed curve in Fig. 4(a) is well reproduced by the model, although the model peak occurs at $X \sim 0.2$ and the observed one at $X \sim 0.35$. In general there is an overestimation of about 25% for $X < 2$. The simulation matches the ground level observations in Fig. 4(b) with a minimal error up to $X \sim 3$. In both cases the observed $\sigma_c/\langle c \rangle$ is constant for $X > 3$, whereas the model $\sigma_c/\langle c \rangle$ tends to zero at large distance from the source.

The underestimation of $\sigma_c/\langle c \rangle$ at large distance is systematic and can also be observed in Fig. 5, which shows the contours of $\sigma_c/\langle c \rangle$ as a function of the dimensionless height and downwind distance. The simulated and observed fields are plotted in Figs. 5(a)

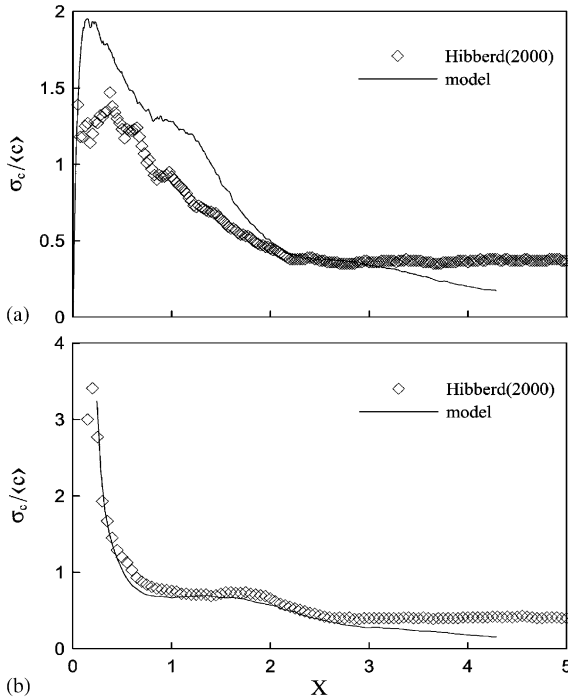


Fig. 4. Intensity of concentration $\sigma_c / \langle c \rangle$ as a function of the dimensionless downwind distance X , measured by Hibberd (2000) (symbols) and modelled (lines); (a) $\sigma_c / \langle c \rangle$ at the plume centre of mass; (b) $\sigma_c / \langle c \rangle$ at the ground level (0.06 h).

and (b), respectively. The simulation is in very good agreement with the observations up to $X \sim 2$ and $z/h \sim 0.8$. However, the experiment shows a constant level of fluctuations at all elevations for $X > 2.5$ whereas the model fluctuations decay to zero. This discrepancy, which was already observed in Fig. 4, is likely to be due to the flux of fluid through the top of the experimental boundary layer as shown in Fig. 2(c). The fluid entering the boundary layer from the top is distributed across the entire vertical domain by the convective turbulence, thus generating fluctuations of concentration σ_c . In addition, the mean concentration $\langle c \rangle$ is also reduced by the intake of fluid. This is probably the only mechanism by which a crosswind line source in a bounded vertical domain can maintain a constant level of fluctuation intensity as clearly observed in Figs. 4 and 5.

The exchange of fluid through the boundary layer top is neglected by our model because of the reflective boundary conditions used in our simulations. More sophisticated boundary conditions such as those suggested by Thomson et al. (1997) should improve the modelling of the upper part of the domain, at the price of additional complexity in the algorithms and slower performances.

Fig. 6 shows the near surface $\sigma_c / \langle c \rangle$ data from the continuous point source release experiments of Dear-

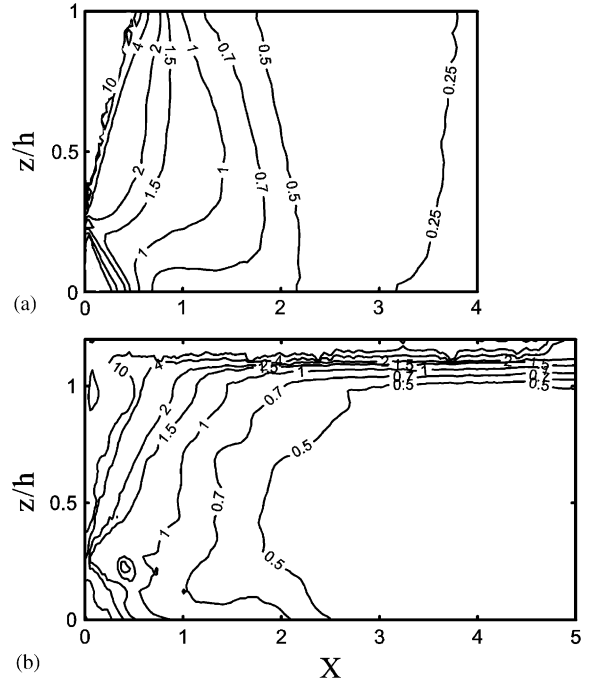


Fig. 5. Contours of intensity of concentration fluctuations $\sigma_c / \langle c \rangle$ for a crosswind line source at $z_s = 0.25 h$. (a) Model simulation; (b) Hibberd (2000) measurements. X is the dimensionless distance and h the CBL height.

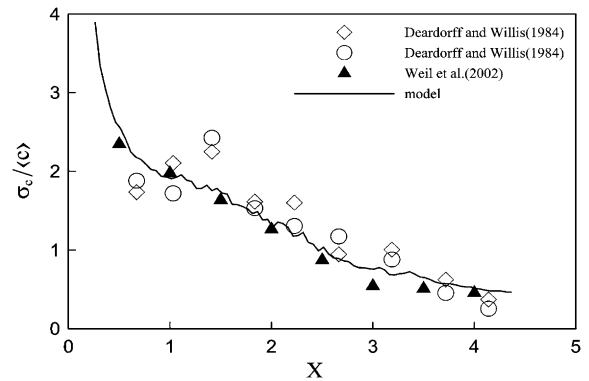


Fig. 6. Modelled and measured ground level concentration fluctuation intensity $\sigma_c / \langle c \rangle$ from a point source at elevation $z_s = 0.22 h$ as a function of the dimensionless downwind distance. The symbol \diamond refers to measured data averaged in the horizontal range $0.5\sigma_y < |y| < \sigma_y$; \circ refers to data averaged in the range $|y| < 0.5\sigma_y$. The model data are averaged over $|y| < \sigma_y$.

dorff and Willis (1984) and Weil et al. (2002) along with our two-dimensional simulation results. The Weil et al. (2002) experiment was intentionally similar to Deardorff and Willis (1984), with the same elevation of release and

stack exit velocity. The source diameter in these experiments was $0.0086h$, which was assumed as the initial spread σ_0 in the simulations.

The data from the Deardorff and Willis (1984) experiment in Fig. 6 were measured at $z = 0.08h$ and are reported as open symbols. The open diamonds refer to the observations averaged over $0.5\sigma_y < |y| < \sigma_y$, the open circles are the data averaged over $|y| < 0.5\sigma_y$. The data of Weil et al. (2002) were measured at $z = 0.05$ along the plume centreline and are reported as solid triangles. The line represents the simulation results at $z = 0.08h$ averaged over $|y| < \sigma_y$. There is an excellent agreement between simulation and experiments. The maximum in the fluctuation intensity at about $X = 1.4$ in the data of Deardorff and Willis was explained and reproduced by a fluctuating plume model in Franzese (2003). The local maximum is due to the raising of the mean plume centreline, in that the fluctuation intensity increases towards the edge of the plume. The effect is partially counterbalanced by the decay of fluctuations with distance. The present model does not describe this maximum and neither do the data of Weil et al. (2002). This suggests that the balance between plume raising and fluctuation decay is sensitive to experimental factors such as type of generation of convection, Reynolds number, distance and permeability of upper and lateral boundaries, and turbulence profiles.

The experiments do not show a constant level of fluctuations at large distance as in the line source experiments of Hibberd (2000) in Figs. 4 and 5. This is probably due to the contribution of the horizontal crosswind component of turbulence to the fluctuation intensity, which is missing in the line source experiments.

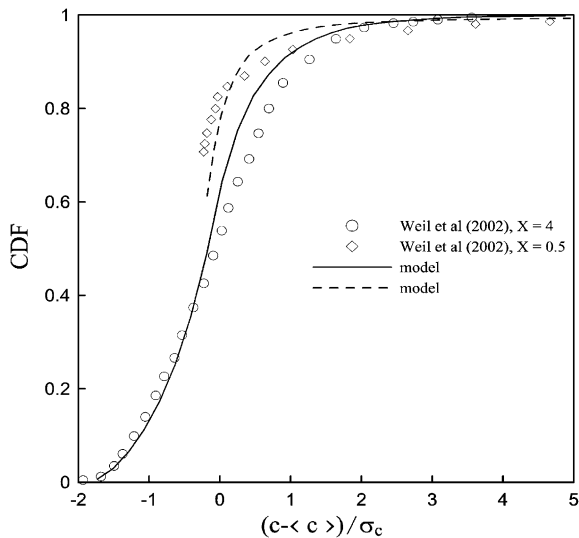


Fig. 7. Measured and modelled cumulative distribution function (CDF) of concentration at two downwind distances from the source.

This contribution tends to zero as the distance increases, causing the steady decay of $\sigma_c / \langle c \rangle$ shown in Fig. 6. However, when the fluctuations generated by the horizontal turbulence become negligible compared to the fluctuations generated by the fluid entrained from the top, we expect to observe a constant level of $\sigma_c / \langle c \rangle$.

The model is able to calculate the full PDF of concentration $f(c)$. The predicted cumulative distribution function is compared to the measurements of Weil et al. (2002) in Fig. 7. The agreement is quite good considering the complexity of the non-homogeneous and non-Gaussian turbulence in the CBL. In Fig. 8 the predicted $f(c)$ are compared with the gamma distributions that Weil et al. (2002) found to correctly fit their data, accordingly to the results of Yee and Chan (1997).

The slight discrepancies between the predictions and the measurements cannot possibly be related to a single model component. An important factor is certainly the

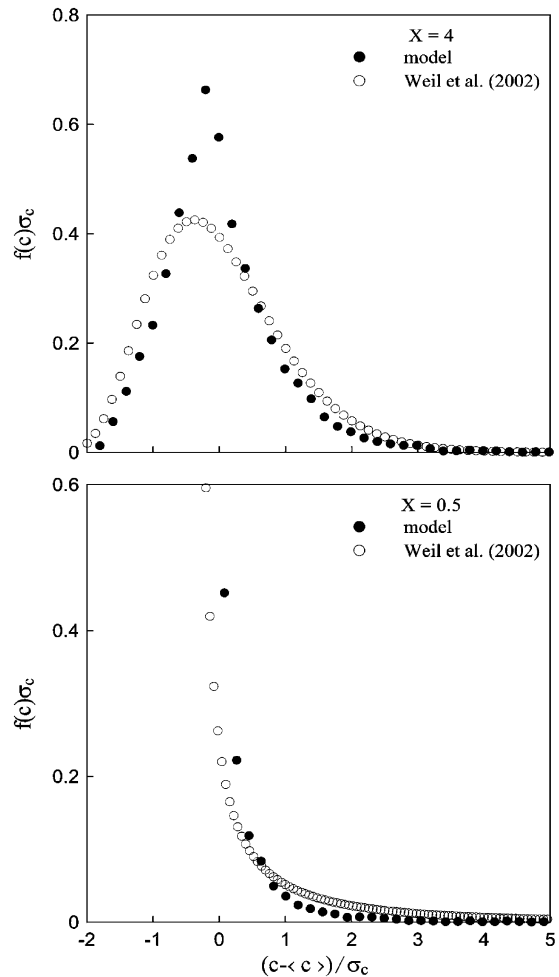


Fig. 8. Probability density function of concentration $f(c)$ predicted by the model along with the best fit Gamma distribution to the data of Weil et al. (2002).

IECM micromixing modelling technique, because of its inability to relax the PDF form towards a Gaussian at large distance, when the statistics of the concentration field are homogeneous.

5. Conclusions

The PDF modelling technique developed in Cassiani et al. (2005) was applied to the prediction of concentration moments and one point PDF of a passive tracer released in the CBL.

The model is implemented using a dynamical time-expandable grid, which allows simulations of releases from localised sources in atmospheric flow within acceptable computational times.

Model simulations for point and line sources were compared with water tank experiments. The comparisons were satisfactory especially in consideration of the complexity of the non-homogeneous, non-Gaussian turbulence of the CBL.

The predictions of concentration statistics for a line source are in good agreement with the observations at short and intermediate distance. However, in the far field the model predicts decaying fluctuation intensity with distance, in contrast with the observed constant intensity. The observed level of fluctuation intensity in the far field was explained as the result of fluid entrainment from the top of the boundary layer. This effect is not currently accounted by the model because of the simple reflective boundary conditions used in these simulations. The model can be improved in this respect by modelling the upper boundary as a porous interface between the CBL and the upper atmosphere.

For point source releases the simulated concentration statistics including mean concentration, concentration fluctuations, and PDF of concentration show a satisfactory agreement with the data measured in two different laboratory experiments. For point source releases the effect of fluid entrainment from the top of the boundary layer on the decay of fluctuations is not apparent at the distances covered by the simulations, possibly because the contribution of the horizontal turbulence to the generation of fluctuations is much stronger than that of the vertical turbulence.

The model was compared with non-reactive scalar data sets, however the model equations can account for chemical reactions with straightforward modifications. Future developments include the model extension to chemically reactive substances and testing with experimental data. Alternative micromixing models will also be considered to overcome the limitations inherent in the current IECM technique, which was found to relax the initial shape of the concentration PDF to the observed shape too slowly (Pope, 2000; Cassiani et al., 2005).

Acknowledgements

We are grateful to Dr. Mark Hibberd for providing his original data set and to Alexandre Radicchi for helpful comments. We also acknowledge Drs. Ashok Luhar and Brian Sawford for sending us a preprint of their paper (2005).

References

- Baerentsen, J.H., Berkowicz, R., 1984. Monte Carlo simulation of plume dispersion in the convective boundary layer. *Atmospheric Environment* 18, 701–701.
- Cassiani, M., Giostra, U., 2002. A simple and fast model to compute concentration moments in a convective boundary layer. *Atmospheric Environment* 36, 4717–4724.
- Cassiani, M., Franzese, P., Giostra, U., 2005. A PDF micromixing model of dispersion for atmospheric flow. Part I: development of the model, application to homogeneous turbulence and neutral boundary. *Atmospheric Environment*. doi:10.1016/j.atmosenv.2004.11.020.
- Deardorff, J.W., Willis, G.E., 1984. Ground level concentration fluctuations from a buoyant and a non-buoyant source within a laboratory convectively mixed layer. *Atmospheric Environment* 18, 1297–1309.
- Deardorff, J.W., Willis, G.E., 1985. Further results from a laboratory model of the convective planetary boundary layer. *Boundary Layer Meteorology* 32, 205–236.
- Fox, R.O., 1996. On velocity conditioned scalar mixing in homogeneous turbulence. *Physics of Fluids* 8, 2678–2691.
- Franzese, P., 2003. Lagrangian stochastic modelling of a fluctuating plume in the convective boundary layer. *Atmospheric Environment* 37, 1691–1701.
- Franzese, P., Luhar, A.K., Borgas, M.S., 1999. An efficient Lagrangian stochastic model of vertical dispersion in the convective boundary layer. *Atmospheric Environment* 33, 2337–2345.
- Gardiner, C.W., 1983. *Handbook of Stochastic Methods for Physics Chemistry and the Natural Sciences*. Berlin, Springer 442pp.
- Hibberd, M.F., 2000. Vertical dispersion of a passive scalar in the convective boundary layer: new laboratory results. In: *Preprints, 11th AMS Conference on the Applications of Air Pollution Meteorology*, American Meteorological Society, Boston, pp. 18–23.
- Hibberd, M.F., Sawford, B.L., 1994. A saline laboratory model of the planetary convective boundary layer. *Boundary Layer Meteorology* 67, 229–250.
- Luhar, A.K., Britter, R.E., 1989. A random walk model for dispersion in inhomogeneous turbulence in a convective boundary layer. *Atmospheric Environment* 23, 1911–1924.
- Luhar, A.K., Hibberd, M.F., Hurley, P.J., 1996. Comparison of closure schemes used to specify the velocity PDF in Lagrangian stochastic dispersion models for convective conditions. *Atmospheric Environment* 30, 1407–1418.
- Luhar, A.K., Hibberd, M.F., Borgas, M.S., 2000. A skewed meandering plume model for concentration statistics in the convective boundary layer. *Atmospheric Environment* 34, 3599–3616.

- Luhar, A.K., Sawford, B.L., 2005. Micromixing modelling of concentration fluctuations in inhomogeneous turbulence in the convective boundary layer. *Boundary Layer Meteorology* 114, 1–30.
- Pope, S.B., 2000. *Turbulent Flows*. Cambridge University Press, Cambridge 806pp.
- Sawford, B.L., 2004. Micro-mixing modelling of scalar fluctuations for plumes in homogeneous turbulence. *Flow Turbulence and Combustion* 72, 133–160.
- Thomson, D.J., 1987. Criteria for the selection of the stochastic models of particle trajectories in turbulent flows. *Journal Fluid Mechanics* 180, 529–556.
- Thomson, D.J., Montgomery, M.R., 1994. Reflection boundary conditions for random walk models of dispersion in non-Gaussian turbulence. *Atmospheric Environment* 28, 1981–1987.
- Thomson, D.J., Physick, W.L., Maryon, R.H., 1997. Treatment of interfaces in random walk dispersion models. *Journal of Applied Meteorology* 36, 1284–1295.
- Weil, J.C., Snyder, W.H., Lawson Jr., R.E., Shipman, M.S., 2002. Experiments on buoyant plume dispersion in a laboratory convection tank. *Boundary Layer Meteorology* 102, 367–414.
- Willis, G.E., Deardorff, J.W., 1976. A laboratory model of diffusion into the convective planetary boundary layer. *Quarterly Journal of the Royal Meteorological Society* 102, 427–445.
- Willis, G.E., Deardorff, J.W., 1978. A laboratory study of dispersion from an elevated source within a modelled convective planetary boundary layer. *Atmospheric Environment* 12, 1305–1311.
- Willis, G.E., Deardorff, J.W., 1981. A laboratory study of dispersion from a source in the middle of the convective mixed layer. *Atmospheric Environment* 15, 109–117.
- Yee, E., Chan, R., 1997. A simple model for the probability density function of concentration fluctuations in atmospheric plumes. *Atmospheric Environment* 31, 991–1002.